STRUCTURAL STABILITY OF ALUMINOSILICATE INORGANIC POLYMERS: INFLUENCE OF THE PREPARATION PROCEDURE

#LIBOR KOBERA, ROMAN SLAVÍK*, DAVID KOLOUŠEK**, MARTINA URBANOVÁ, JIRI KOTEK, JIRI BRUS

Institute of Macromolecular Chemistry, Academy of Sciences of the Czech Republic,
Heyrovsky sq. 2, 162 06 Prague, Czech Republic
**Faculty of Technology, Tomas Bata University in Zlin,*
sq. T. G. Masaryka 275, 762 72 Zlin, Czech Republic
***Institute of Chemical Technology Prague, Technicka 5, 166 08 Prague, Czech Republic*

#E-mail: kobera@imc.cas.cz

Submitted May 20, 2011; accepted September 18, 2011

Keywords: Aluminosilicate inorganic polymers, Solid-state NMR, Phase transformation

The stability of amorphous aluminosilicate inorganic polymer (AIP) systems with regard to the structural role of water molecules incorporated in inorganic matrix is discussed. Innovative approach to preparation of amorphous AIP systems with identical chemical composition but differing in structural and mechanical behavior is introduced. It is shown that even small changes in the manufacture dramatically affect mechanical properties and the overall structural stability of AIP systems. If the required quantity of water is admixed to the reaction mixture during the initial step of AIPs synthesis the resulting amorphous aluminosilicate matrix undergoes extensive crystallization (zeolitization). On the other hand, if the amount of water is added to the reaction mixture during the last step of the preparation procedure, the inorganic matrix exhibits long-term stability without any structural defects. To find the structural reasons of the observed behavior a combination of traditional solid state NMR (^{1}H and ^{29}Si MAS NMR, ^{29}Si CP/MAS NMR, ^{29}Si inverse-T1-filtered NMR), XRPD and TGA measurements were used. The applied experiments revealed that the structural stability of AIPs can be attributed to the tight binding of water molecules into the inorganic matrix. The structural stability of the prepared amorphous AIP systems thus seems to be affected by the extent of hydration i.e. the strength of binding water into the inorganic framework.

INTRODUCTION

Although the layered aluminosilicate minerals are widely used as a raw material that has found a wide application in industry and material science, their potentiality has not been fully exploited yet. Consequently new applications and technologies are currently under deep investigation. Among others, clay minerals are used as a suitable source for the preparation of aluminosilicate inorganic polymers (AIP) that exhibit increasing industrial interest, due to the low energy requirements of their manufacture and their promising mechanical properties (compression strength, heat and chemical resistance, etc.). The first preparation of inorganic polymers was carried out in the 1950's by Gluchovskij [1]. In the subsequent years, Davidovits [2] proposed new terminology and described the process of preparing aluminosilicate inorganic polymers (geopolymers) as well as their properties in detail [2-8]. One of the most attractive features of these materials is that waste materials like colored low-quality kaolin, fly ash or slag [9-12] can be used for their manufacture, opening thus new solutions of many environmental problems. AIP materials can also be used as new types of cements, concretes [3,13-15], ceramics, toxic waste storage materials [2,4,10,11,16], special biomaterials [17] and fiber reinforced composites [2,4,18].

In general, AIPs are formed through the reaction of calcinated aluminosilicates with alkali solutions (Na/K hydroxide solutions or Na/K activated sodium silicate). The reaction usually proceeds at atmospheric pressure and ambient temperature. During the reaction the decomposition of calcinated aluminosilicate is initiated and subsequent rearrangement of aluminum species and their polycondensation with siloxane tetrahedra leads to the formation of a three-dimensional network of Si–O–Al motifs [2,4,5,19-22]. The elementary building units of the prepared network consist of fully condensed silica tetrahedra $Q^4(n\mathrm{Al})$, where n, ranging between 0 and 4 reflects the extent of Al-for-Si substitution in the second coordination sphere. In some cases a limited extent of incomplete polycondensation of silanol groups was observed. This leads to the presence of a small amount of hydroxyl-substituted Q^2 and Q^3 units in the final products [23,24]. Consequently, the AIPs are complex amorphous or semi-crystalline materials. This fact gives rise to specific requirements regarding the thorough structural characterization of these materials.

In many cases the combination of X-ray powder diffraction (XRPD) and solid-state NMR spectroscopy is required. While XRPD can easily describe mineralogical composition, solid state NMR gives information on the structure of amorphous phases. From a chemical point of view, AIPs can be divided into two classes depending on the activation agent used: *i*) the sodium systems, activated by NaOH; *ii*) the potassium systems, activated by KOH. Although the K-systems show better mechanical properties, the Na-systems are economically much more advantageous [5,6].

In our previous work [25] we introduced new types of alternative AIP systems based on the preparation of a reactive AIP precursor by the direct calcination of low-quality kaolin with solid Na/K hydroxides. Among others, it was found out that in some cases the prepared amorphous AIPs are not stable and undergo extensive rearrangement (crystallization and formation of zeolite domains). Besides the observed structural changes and formation of zeolite fractions significantly affected mechanical properties.

It has been already reported that short-range order and crystallinity of the prepared AIP systems can be controlled by the chemical composition of reaction mixtures and/or conditions of their preparation [26-32]. In general, the degree of crystallinity of the resulting AIPs is decreased when a solution of sodium silicate is used instead of a solution of alkali hydroxide [26]. Amorphous systems are formed especially at higher concentration of silicates in the activation solutions [31] where Na^+ ions are not fully hydrated [32]. Up to date, however, a comprehensive description of the processes and factors inducing crystallization of amorphous AIP systems was not reported.

Therefore we focused our research on the fundamental aspects of the amorphous-crystalline phase transition occurring in these inorganic polymers. In order to better understand this process and to find the key factors that control the undesired crystallization of AIP systems we tested a wide range of syntheses of AIPs described in literature [17,19,33,34]. From the preliminary screening we selected the most representative ones and the resulting materials were subjected to the detailed structural investigation using ss-NMR, XRPD, TGA and artificial aging. To reduce the number of parameters that can be varied during the preparation of AIP systems we kept the final chemical composition of reaction mixture always constant.

EXPERIMENTAL

Materials

The investigated systems were prepared from kaolin (Sedlec quarry, Czech Republic) calcinated at 750°C for 6 hours, with the chemical composition determined by X-ray fluorescence (XRF) of 51.16 % SiO_2, 45.59 % Al_2O_3. The size of metakaolin particles, determined by the grain size analysis, was 0.125 mm. As a binding agent, sodium metasilicate R-145 (Zaklady Chemiczne Rudniki S.A., Poland) with the chemical composition 40.3 % SiO_2, 17.4 % Na_2O, 42.3 % H_2O, was used, and sodium hydroxide (Lach-Ner, Neratovice, Czech Republic) was applied as activator.

The total composition of reaction mixtures was always the following: 70 g of metakaolin, 52 g of water glass, 8.5 g of NaOH and 19.5 g of H_2O, resulting in the ratios: $SiO_2/Al_2O_3 = 3.2$, $Na_2O/Al_2O_3 = 1$, $H_2O/Na_2O = 8$. The amounts of the used components and total amount of water correspond with the generally accepted composition of typical AIP systems [11,32,35,36].

Synthesis of AIP systems

Two procedures were followed to prepare AIP systems with different structural behavior and properties (phase-stable and phase-unstable systems, Fig. 1).

Synthesis of the Stable AIP system (Method A):

To prepare a stable AIP system (thereafter referred as phase-stable system) the aqueous solution of sodium metasilicate (Na_2SiO_3, as purchased) was activated by powdered sodium hydroxide (step 1a, Fig. 1). The mixture was then let to stand in the closed vessel for 48 hours. In the next step, finely powdered calcinated kaolin (metakaolin) was added into the activated solution of Na_2SiO_3 and the whole mixture was homogenized for 45 minutes in a kneader with star stirring and planetary circulation. At the end of this period the resulting product exhibited gel-like consistence (step 2a, Fig. 1). In the third step, the corresponding amount of water was added to the mixture to reach required chemical composition (step 3a, Fig. 1). Then the obtained mixture was mixed for 30 minutes (step 4a, Fig. 1). Finally the resulting homogeneous paste was placed into the Teflon mold to create testing specimens. To remove air bubbles that can be entrapped it the prepared paste the Teflon mold was placed on a vibration table and vibrated 10 min, (step 5a, Fig. 1).

Synthesis of the Unstable AIP system (Method B):

A very similar procedure was used to prepare an unstable AIP system (thereafter referred as phase-unstable system). The difference in the applied preparation techniques lies in the activation period, when in the case of Method B solution of sodium metasilicate (as purchased) was activated by the aqueous NaOH (step 2b, Fig. 1). After the activation period (48 hours) the required amount of metakaolin was added into the mixture that was further mixed to reach homogenous consistence (75 minutes, step 3b, phase-unstable system, Fig. 1). The testing specimens were prepared by the same procedure as described above.

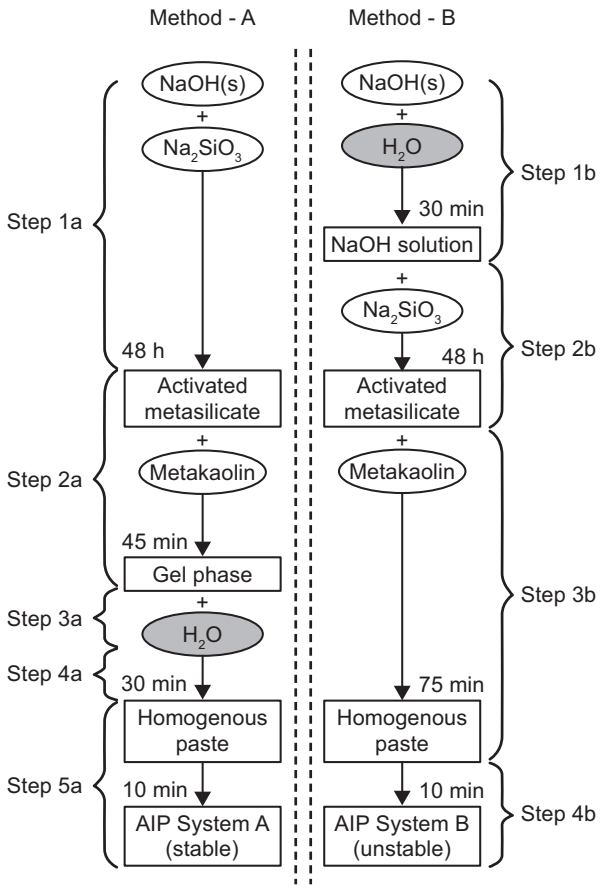

Figure 1. Preparation of phase-stable (A) and phase-unstable (B) AIP systems in a graphical representation (left and right, respectively). The difference between both procedures lies in the moment of the addition of water into the reaction mixture. This point is highlighted by grey ellipsis.

Preparation of testing specimens and treatment conditions

The testing specimens (cylinders with diameter = 1.5 cm and height = 3.0 cm) prepared from the paste resulting from the above procedures, were put to stand for 7 days at ambient temperature and atmospheric pressure. After 7 days, one half of the prepared samples was tested while the remaining samples were artificially aged. The artificial aging (the samples were placed in a Teflon-lined autoclave and kept at constant temperature 140°C for 14 days) was used to accelerate structural transformation that can occur in amorphous phase of the prepared AIP systems.

Model experiments: activation periods of sodium metasilicate

Since the applied methods of preparing stable and unstable AIP systems differ in the activation of sodium metasilicate this period was probed in detail separately. To reach this goal the model reaction mixtures was prepared and chemical reactions were followed by ^{29}Si MAS and CP/MAS NMR spectroscopy. The model reaction systems were prepared as follows:

1) Solution of sodium metasilicate (35 g, as purchased) was activated by powdered NaOH(*s*) (6.6 g). This resulted in the ratios: $Si/Na^+ = 0.62$, $H_2O/Na^+ = 4.8$. The prepared reaction mixture (referred as MS_A) thus represents the activation period of the synthesis of phase-stable (step 1a, Figure 1).
2) Solution of sodium metasilicate (35 g, as purchased) was activated by aqueous solution of NaOH(*aq*) (16.3 g = 9.7 g H_2O + 6.6 g NaOH(*s*)). This resulted in the ratios: $Si/Na^+ = 0.62$, $H_2O/Na^+ = 8.0$; and the prepared reaction mixture (referred as MS_B) represents the activation period of the synthesis of phase-unstable (step 1b + 2b, Figure 1).
3) As a reference polycondensation of sodium metasilicate without any activator (MS_0) was also monitored.

Since polycondensation of silanol groups is equilibrium reaction that requires consumption of low-molecular-weight byproducts [22] all the prepared mixtures were placed in Petri dishes under laboratory conditions (atmospheric pressure and ambient temperature). Although the activation period usually takes 2 days the model mixtures were monitored over 55 days in order to reach final stages of reactions. The course of depolymerisation and subsequent polycondensation reactions was quantitatively expressed by the degree of condensation

$$q_i = \sum_{n=1}^{4} nQ^n/4,$$

where Q^n is the mole fraction of each siloxane Q^n structure unit and n denotes the number of silicon atoms surrounding the central SiO_4 unit.

Analytical techniques

Compression tests of the prepared AIP systems before and after the accelerated aging were performed. Compression strength values were determined using a universal testing machine INSTRON 5800R model 6025, with speed 5mm/min.

NMR spectra were measured at 11.7 T using a Bruker Avance 500 WB/US NMR spectrometer equipped with double-resonance 4-mm and 2.5-mm probeheads. ^{1}H MAS NMR spectra were acquired at 500.182 MHz, spinning frequency was $\omega_r/2\pi = 25$ kHz; 90° pulse width was 2.5 μs; and recycle delay was 2 s. ^{29}Si MAS NMR spectra were acquired at 99.325 MHz; spinning frequency was $\omega_r/2\pi = 7$ kHz; 90° pulse width was 4 μs and recycle delay was 10 s. The extend of hetero-polycondensation involving SiO_4 and AlO_4 tetrahedra was probed by the inverse-T_1-filtered ^{29}Si MAS NMR experiment which consists of a train of 90° pulses separated by variable repetition delay (RD) ranging from 60 to 1 s (Figure 2).

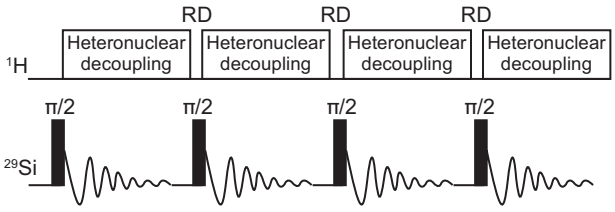

Figure 2. Schematic representation of the inverse-T_1-filtered ^{29}Si MAS NMR experiment. Recycle delay (RD) was varied from 1 to 60 s.

^{29}Si MAS and CP/MAS NMR spectra of model reaction mixtures (liquids, gels and solids) were measured in ZrO_2 spacers [37,38]. The first sampling was performed at zero time and the second sample was taken from the mixture 30 minutes after the mixing of all components. Subsequently the reaction mixtures were sampled after 3, 9, 48 hours and 6, 27 and 55 days. Taking into account frictional heating of the samples during fast rotation all NMR experiments were preformed at 308 K. Temperature calibration was performed on $Pb(NO_3)_2$ using a procedure described in literature [39].

Powder X-ray diffraction data were recorded using 3000P Seifert instrument (Germany) using CoK_α radiation. Each sample was measured between 6-70° 2Θ (step 0.05° 2 Θ/s) for qualitative identification of individual phases. For quantitative identification each sample was measured 3-times with step 0.02 °2 Θ/s.

Weight losses of finely powered samples of AIP systems were monitored by thermogravimetric analysis (TGA) using a Perkin-Elmer instrument. The samples (ca. 10 mg) were placed on a platinum pan and heated up to 350 °C at 3 °C/min under nitrogen atmosphere (flow rate 50 ml/min). In order to avoid contamination by the air humidity the samples were stored in closed desiccator.

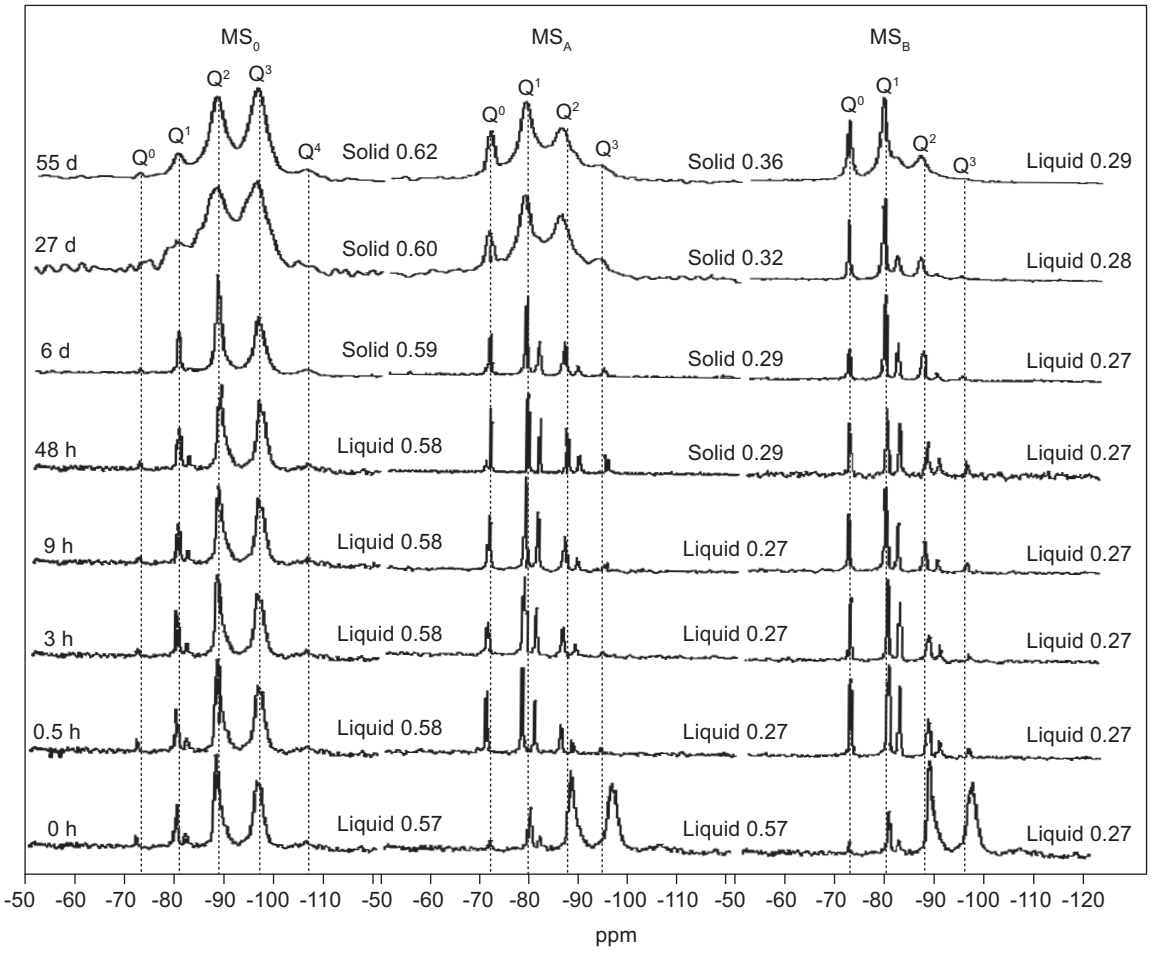

Figure 3. ^{29}Si MAS NMR spectra of model metasilicate solutions recorded during the activation period (48 hours) and subsequent polycondensation (55 days). Free polycondensation of non-activated sodium metasilicate solution (MS_0); polycondensation of sodium metasilicate solution activated by solid NaOH(s) (MS_A); and polycondensation of metasilicate solution activated by aqueous solution of NaOH(aq) (MS_B).

RESULTS AND DISCUSSION

Activation period of AIP synthesis

In general, alkali activation of sodium metasilicate solution by NaOH leads not only to the adjustment of silicate modulus (i.e. SiO_2/Na_2O ratio) which should be between 1 and 2, but also initiates depolymerisation of metasilicate (siloxane) oligomers. The depolymerisation, for both model systems (MS_A and MS_B), was completed within 30 minutes as the broad signals of Q^3 and Q^2 units of primary metasilicate disappeared and new narrow signals appeared in the high-frequency region (see ^{29}Si MAS NMR spectra, Figure 3). The narrow signals resonating at -70, -78, -81, -87, -89, -96 ppm can be attributed to the Q^0, Q^1, Q^2 structure units of monomers, dimers and other short oligomers, respectively [40,41].

Subsequent polycondensation and formation of polysiloxane network is very slow as condensation degree only slightly increases. This is reflected by the increase in intensities of signals of Q^2 and Q^3 units. During the first 48 hours the condensation degree slightly increases from 0.27 to 0.29 (Figure 3). However, and quite surprisingly, just at this moment the system activated by solid NaOH (model system MS_A) solidifies and transforms from liquid state to cloudy solid material. On the other hand, the system activated by aqueous NaOH (model system MS_B) as well as non-activated metasilicate solution (reference system MS_0) remains clear viscous liquids. As indicated by the low condensation degree reached after 48 hours (q_i=0.29), the observed solidification of MS_A must results from physical aggregation of SiO_4^{4-} tetrahedra that is governed by ionic interactions. To confirm the existence of these aggregates and to identify their chemical nature the ^{29}Si CP/MAS NMR experiments were performed. The advantage of these ^{29}Si CP/MAS NMR experiments follows from the fact, that only rigid molecular fragments surrounded by hydrogen atoms can be effectively detected, while the proton free or highly mobile siloxane units do not provide NMR spectra.

Figure 4 (right) shows the ^{29}Si CP/MAS NMR spectra of MS_A system in the time period from 2 to 55 days, and the detectable signal was recorded just after 48 hours. On the basis of its chemical shift (-70 ppm), the recorded signal can be assigned to monomeric (SiO_4^{4-}) silica tetrahedra (non-condensed, Q^0 structure units), that with high probability aggregate together with water molecules and Na^+ ions to form microcrystals of sodium silicate hydrate ($Na_2SiO_3 \cdot H_2O$) [41]. At later stages of chemical reaction the signal intensity as well as linewidth slightly increases. Barely detectable signals of Q^1, Q^2 and Q^3 units resonating at -78, -88 and -96 ppm were detected after 55 days indicating formation of secondary polymer network. On the other hand, in the ^{29}Si CP/MAS NMR spectra measured for sodium metasilicate activated by aqueous NaOH(*aq*) (MS_B) no signals were recorded even after 55 days (the spectra are not presented). This indicates that in the dissolved system no aggregation of silica tetrahedra occurs. In addition, formation of polysiloxane network is also limited. Creation of such network requires much lower pH as demonstrated on the polycondensation of non-activated sodium metasilicate (referential system, MS_0). The primary fragments of this immobilized, highly branched polysiloxane network

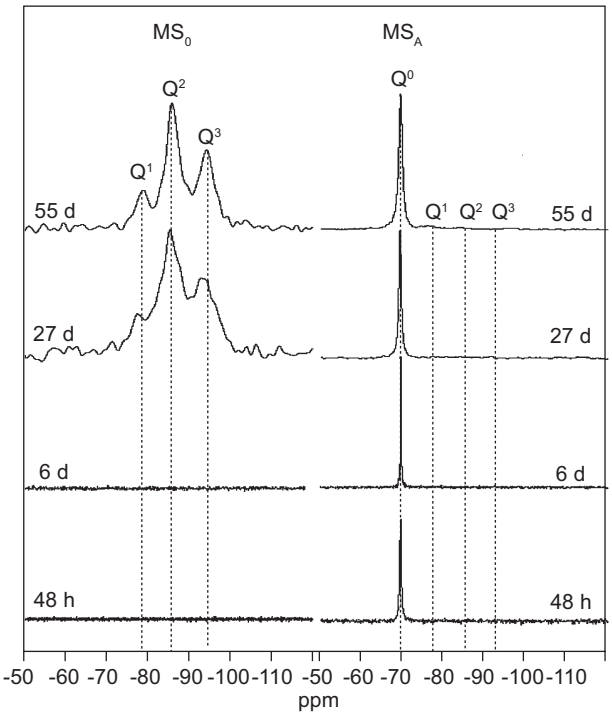

Figure 4. ^{29}Si CP/MAS NMR spectra of non-activated metasilicate solution (MS_0); and metasilicate solution activated by solid NaOH (MS_A) recorded at various stages of solidification.

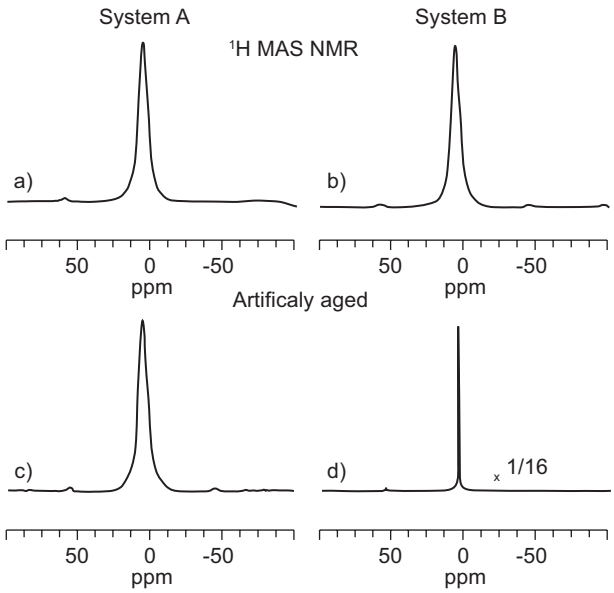

Figure 5. ^{1}H MAS NMR spectra of the phase-stable system before a) and after accelerated aging c); and the corresponding spectra of the phase-unstable AIP system before b) and after accelerated aging d).

were detected in the ^{29}Si CP/MAS NMR spectrum after 27 days of polycondenstaion as the broad signals resonating at -80, -85 and -95 ppm.

In general, reaction mechanism under which silica tetrahedra (SiO_4^{4-}) mutually interact (either by covalent bonding - polycondensation, or by ionic bonding - aggregation) is governed by Si/Na^+ ratio, since the presence of alkaline cations has to be balanced electrostatic. Non-condensed silica units have a larger negative charge (per Si atom) than the condensed ones. Thus, the increase in the concentration of Na^+ ions causes the decrease in the rate of silica condensation. Consequently the aggregation of silica tetrahedra (SiO_4^4) is preferred in the activated systems with very high pH. This is in agreement with our observation only partly because in both the activated systems, MS_A as well as MS_B, the Si/Na^+ ratio is identical ($Si/Na^+ = 0.62$). Aggregation, however, occurs only in MS_A system. Therefore, we suggest that the observed inability of silica units to aggregate in MS_B is caused by the high amount of water in the system. With high probability, just the amount of water responsible for hydration of Na^+ ions, has substantial effect on the strength of electrostatic forces and thus on the tendency to aggregation of silica units. From these findings follows that basic structural fragments, certain pre-aggregates of silica tetrahedra with tightly incorporated sodium ions and water molecules and can be predetermined even at the end of activation period. In our particular case we can expect formation of these compact pre-aggregates during the activation sodium metasilicate by powdered NaOH(*s*), while in the dissolved system of Na_2SiO_3 activated by NaOH(*aq*), in which sodium ions are fully hydrated, silica terahedra rather remain free and effectively isolated. The influence of these differences (different activation of sodium metasilicate) on the properties of the prepared AIP systems (Figure 1) is probed in detail the following sections.

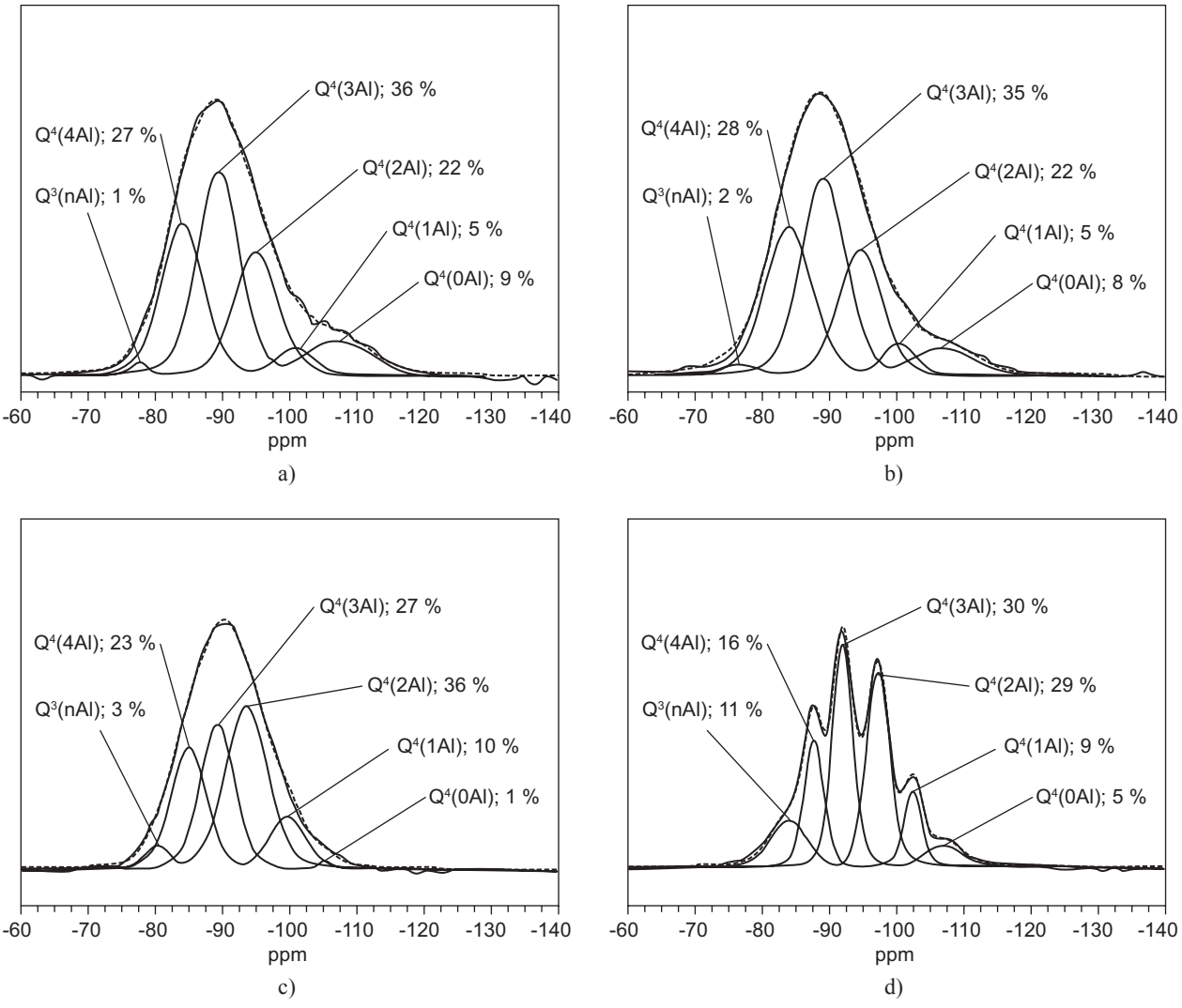

Figure 6. ^{29}Si MAS NMR spectra of the phase-stable system before a) and after accelerated aging c); and the corresponding spectra of the phase-unstable AIP system before b) and after accelerated aging d).

Mechanical properties of AIP systems

Primary information on the quality and structural integrity of the prepared AIP systems was obtained from the standard measurements of compression strength. Before the accelerated aging both AIP systems exhibited the same compression strength values of about 65-67 ± 5 MPa. This indicates that both syntheses (Method A and B) allow the same rate of chemical conversion of metakaolin. On the other hand, the prepared AIP systems show significantly different behavior after the accelerated aging. While the phase-stable system exhibits unaltered mechanical strength of about 69 ± 5 MPa, the compression strength values of the treated phase-unstable system is reduced to ca 55 % of the original value (37 ± 5 MPa) indicating thus progressive phase transformation.

Structure of AIP systems

To get a deeper insight into the structure of AIP materials the XRPD analysis and solid-state NMR spectroscopy (ss-NMR) are ones of the most suited methods. In agreement with the mechanical testing no differences between the prepared stable and ustable systems were found in ^{1}H and ^{29}Si MAS NMR spectra recorded (Fig. 5 and 6, upper spectra). Both systems provide identical NMR spectra predominated by a single broad signal centered around 5 and -87 ppm for ^{1}H and ^{29}Si nuclei, respectively. These findings confirm that both syntheses (Method A and B) allow the same, basically complete rate of polycondensation of AlO_4 and SiO_4 tetrahedra leading to the formation of a typical well-evolved amorphous aluminosilicate network. Also the patterns of XRPD exhibit very similar broad signal

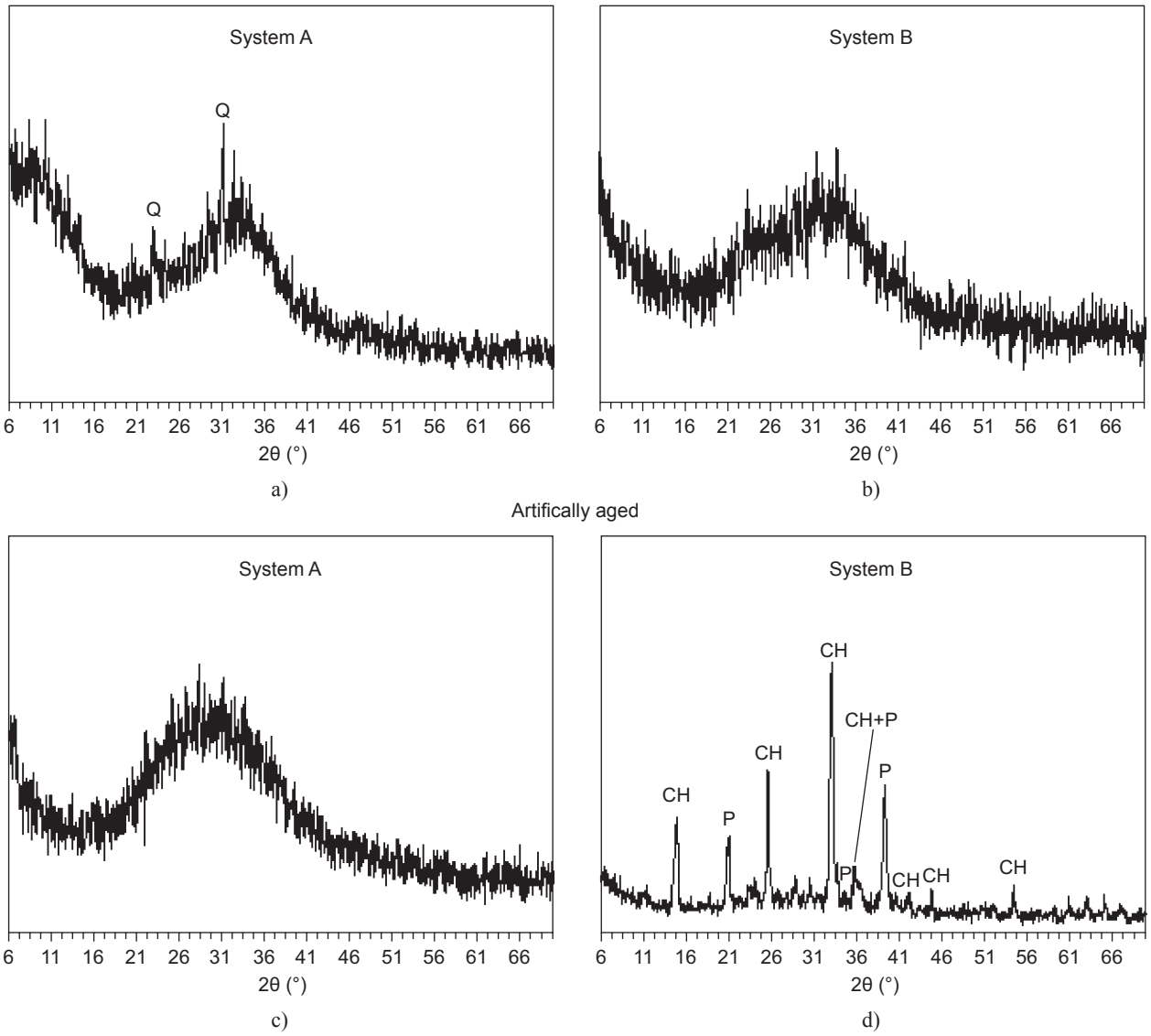

Figure 7. XRPD patterns of the phase-stable system before a) and after accelerated aging c); and the corresponding spectra of the phase-unstable AIP system before b) and after accelerated aging d).; Q = quartz (< 1 %), CH = Chabasite (~45%), P = Zeolite P (~30%).

centered at 31° 2Θ, and thus prove the high degree of transformation of metakaolin to amorphous system. Residual traces of quartz (< 1%) were found in the stable system (Figure 7).

Despite the recorded ^{1}H and ^{29}Si MAS NMR spectra did not show significant difference between the prepared systems, detail analysis of NMR signals provided basic structural information. In ^{1}H MAS NMR spectra both systems phase-stable and phase-unstable are represented by nearly identical broad NMR signals (half-width 3.5 kHz) at ca. 5 ppm. The linewidth as well as chemical shift of these signals indicate relatively strong binding of water molecules into the inorganic matrix (Fig. 5, upper spectra), which as indicated by nearly featureless ^{29}Si MAS NMR spectra (Figure 6), consists of a broad distribution of aluminosilicate building units $Q^4(n\mathrm{Al})$ (n=0-4;) without significant long-range and short-range order. The signal decomposition revealed that the most abundance species are Q^4(4Al) and Q^4(2Al) units (27 and 22 % respectively). In addition to heteropolymer motifs (Si–O–Al) a small fraction (ca. 8%) of homopolymer Si–O–Si segments represented by Q^4(0Al) species were found in both AIP systems (Figure 6).

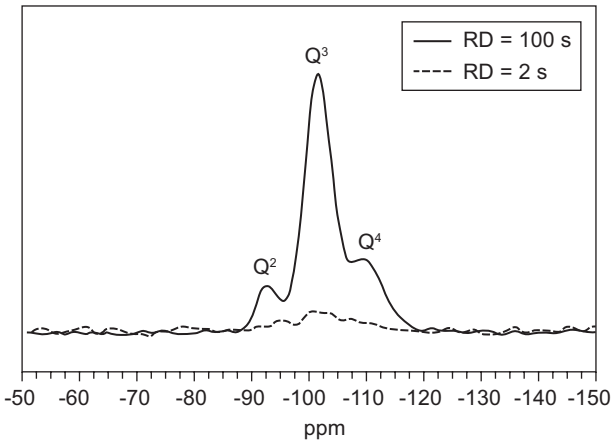

a)

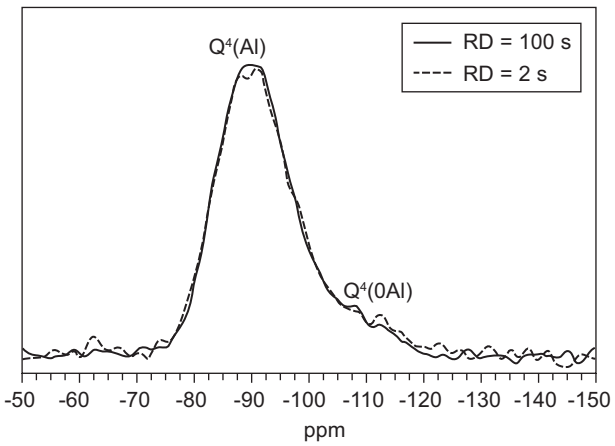

b)

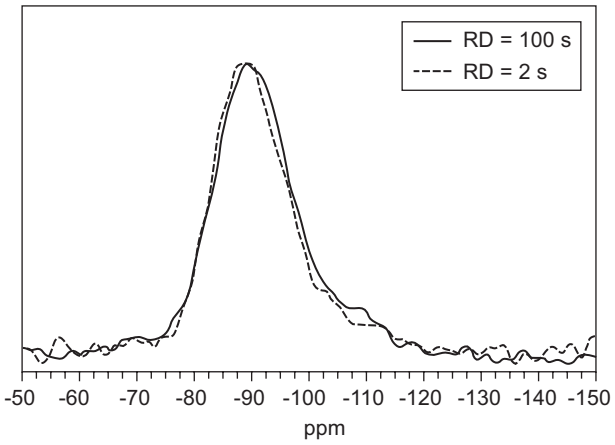

c)

Figure 8. Inverse T1-filtered 29Si MAS NMR spectra of amorphous silica; the prepared AIP systems A and B recorded with RD = 2 s (dashed line) and RD = 100 s (black line).

The coexistence of homopolymer and heteropolymer fragments opens the question of structural homogeneity of the prepared systems. Homopolymer fragments can in principle form either large phase-separated domains of amorphous SiO_2 and/or small star-like clusters Q^4(0Al) that are regularly combined with Q^4(1-4Al) units. Regarding this issue we performed the inverse-T_1-filtered ^{29}Si MAS NMR experiment with variable recycle delay ranging from 1 to 60s. This technique is based on the assumption that T_1 relaxation of ^{29}Si spins in large domains of Q^4(0Al) units are extremely slow and recording of ^{29}Si NMR spectra requires long repetition delay. On the other hand, regular combination of Q^4(0Al) clusters with AlO_4^- tetrahedra accelerates T_1 (^{29}Si) relaxation to such extend that high-quality NMR spectrum can be recorded with very short repetition delay.

To verify this assumption we perform tests on amorphous silica prepared by acid catalyzed polycondensation of tetraethoxysilane (TEOS) that can be considered as a model of large phase-separated domains of Q^4(0Al) (Figure 8). In this particular case the ^{29}Si NMR signals of Q^4 structure units are not fully equilibrated even after the longest recycle delay (100s) applied. On the other hand, in the case of the prepared AIP systems the ^{29}Si MAS NMR signal centered at -106 ppm corresponding to Q^4(0Al) species was recorded with equilibrium (non-reduced) intensity using a very short repetition delay of 2 s. This finding thus confirms that Q^4(0Al) structure units do not form large domains in the prepared AIP systems, and rather the central Si atom is surrounded by Al atoms in the fourth coordination sphere forming –Si–O–Si–O–Al– fragments.

Phase transformationand structural changes

Dramatic changes in the structure of AIP systems were induced by the accelerated aging, and the originally hidden differences between the phase-stable and phase-unstable systems are now clearly apparent in ^{1}H, ^{29}Si

MAS NMR spectra (Fig. 5 and 6, lower spectra). After the artificial aging the ^{1}H MAS NMR signal of the phase-unstable system is extremely narrowed below 100 Hz while the ^{1}H MAS NMR signal of the phase-stable system is unchanged. This finding indicates dramatic changes in mobility of proton species. Originally incorporated water molecules are displaced from amorphous phase, during accelerated treatment, to newly forming channels and are released from inorganic matrix. Similarly ^{29}Si MAS NMR spectra demonstrate structural rearrangement of aluminosilicate matrix. While the ^{29}Si MAS NMR signals of phase-stable system remained broad and featureless, the accelerated aging of phase-unstable system led to the splitting of the originally broad ^{29}Si MAS NMR signal. This indicates permanent amorphicity of the stable phase-stable system, while the phase-unstable system underwent a substantial rearrangement of silica tetrahedra towards a semi-crystalline aluminosilicate framework.

The amorphous-crystalline phase transition is clearly confirmed by narrow reflections in XRPD patterns that can be attributed to the considerable formation of Chabasite and Zeolite P (gismondine type) in the unstable phase-unstable system (Fig. 7, lower spectra). The amount of the formed zeolite fractions, however, does not fully corresponds to the observed changes in the ^{29}Si MAS NMR spectrum, and a broad diffusive reflection, that represents ca. 25% of amorphous phase, is still observed. This means that besides the microcrystalline phase providing sharp X-ray reflections, the nanometer-sized crystalline structures that are too small to provide clear X-ray reflections are also formed.

As indicated by the increase in signal intensities of $Q^3(n\mathrm{Al})$ units the process of redistribution of silica tetrahedra is associated by the cleavage of Si-O-Al bonds. A part of these newly formed Si-OH silanol groups remains uncondensed reducing thus the average network density. Particularly in the unstable phase-unstable system the increase in the amount of $Q^3(n\mathrm{Al})$ units is considerably high reaching up to 11%. This cleavage thus can be the source of reduced compressive strength. On the other hand, in the treated phase-stable system only a slight shift of ^{29}Si MAS NMR signal toward low frequency was observed (to -90 ppm). This change can be explained by the local rearrangement of SiO_4 and AlO_4 tetrahedra that is governed by the decomposition of homopolymer clusters $Q^4(0\mathrm{Al})$. The released SiO_4 units are then incorporated into the aluminosilicate network giving rise copolymer clusters predominated by $Q^4(2\mathrm{Al})$ fragments at the final stage of the process.

Thermogravimetric Analysis (TGA)

Since water molecules, as forming the hydration shell of Na^+ ions, provides a medium that helps to compensate negative charge of AlO_4^- tetrahedra, the water activity in determining the properties of the inorganic polymers cannot be neglected. Primary structural information has been derived form ^{1}H MAS NMR spectra (Figure 5). To get additional data about the binding properties of water molecules thermogravimetric analysis was performed (Figure 9).

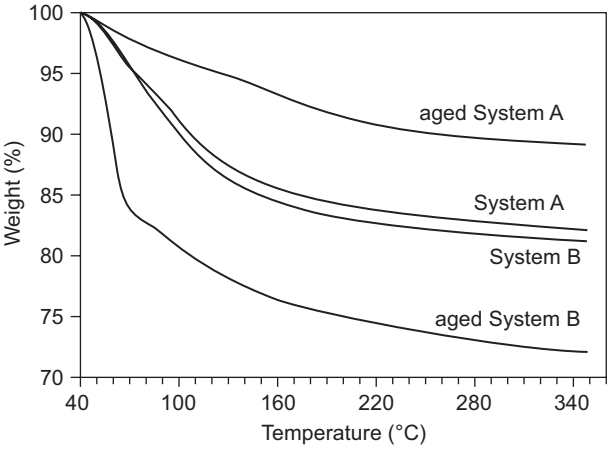

Figure 9. Thermogravimetric (TG) curves of System A and B before and after the accelerated aging.

Both systems (phase-stable and phase-unstable, respectively) exhibit nearly the same TG curves that can be divided into two parts. In the temperature range from 40 to 150°C both the systems liberate molecular water rapidly, while in the second temperature region (150-350°C) the escape of water is significantly slowed down. Although the total weight loss is almost identical in both cases (ca. 17 %), the phase-stable system exhibits slower release of water molecules. This fact indicates stronger interaction between water molecules and aluminosilicate matrix comparison to the phase-unstable system. These differences are highlighted by accelerated aging. After the accelerated aging the rate of water escape as well as the total weight loss (ca. 10 %) is significantly reduced in the phase-stable system . In contrast, the enhanced water evaporation leading to the total weight loss of about 30% is observed in the phase-unstable system. Especially in the temperature range 40 – 75°C the rate of water escape is dramatically enhanced. These findings indicate that the tightly incorporated water molecules are partly inaccessible and cannot be completely removed from the phase-stable system. During the rearrangement of aluminum and silica tetrahedra induced by the accelerated aging the originally partly opened pores (large rings, clusters) are closed down capturing thus water molecules and sodium ions definitively. On the other hand, redistribution of SiO_4 and AlO_4 terahedra in the phase-unstable system leads to formations of large rings and complete opening of these pores. Water molecules then release the stable positions, become labile and as a liquid fill large pores and channels.

Arrangement of water molecules

To obtain detail information on arrangement of water molecules and structural behavior of all proton sites in the prepared systems we performed $^{1}H–^{1}H$ correlation experiments (Figure 10). In general the proton sites in AIP systems involve water molecules, silanol groups, bridging hydroxyls etc., that all of them slightly differ in acidity, strength of hydrogen bonding, chemical surroundings and many other factors. Therefore their ^{1}H NMR signals cover wide spectral width and thus it is very difficult to distinguish between them. So it is not surprising that the $^{1}H–^{1}H$ MAS NMR correlation spectra of both AIP systems reflect a broad variety of proton sites bound to aluminosilicate matrix (Figures 10a and 10b).

However, due to the significantly enhanced spectral resolution of 2D spectra as compared with 1D ones, clear differences between the prepared AIP systems can be identified. Predominantly the high-frequency signal resonating at 14-16 ppm was found in the phase-stable system (Figure 10a). This signal can be assigned protons (H_2O or –OH) exhibiting very strong hydrogen bonding [42-44]. In addition, the detected off-diagonal correlation signals (at ca. 10 and 5 ppm) and their intensities indicate that the majority of hydroxyls and water molecules mutually interact by dipolar couplings forming thus a large interaction network (clusters). With high probability these protons (water molecules, –OH groups etc.) are mutually hydrogen-bonded [42-44]. On the other hand, the absence of the high-frequency

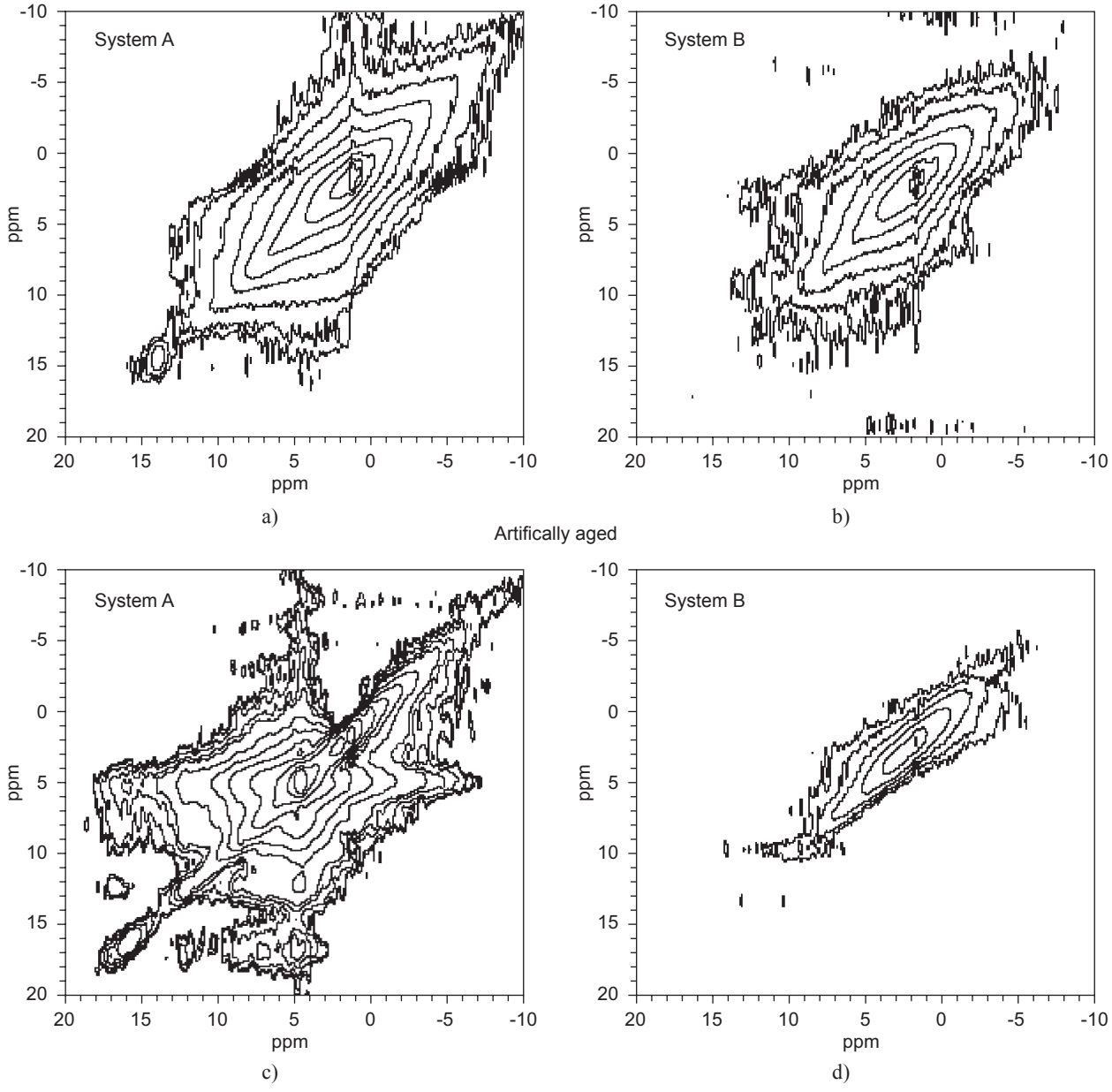

Figure 10. $^{1}H–^{1}H$ MAS NMR correlation spectra measured with a mixing period 25 ms of the phase-stable system before a) and after accelerated aging c); and the corresponding spectra of the phase-unstable AIP system before b) and after accelerated aging d).

^{1}H NMR signal and the lack of off-diagonal correlation signals in the ^{1}H-^{1}H MAS NMR spectrum indicates much weaker interactions between the protons in the phase-unstable system (Figure 10b). In this case it can be assumed that formation of clusters of hydrogen-bonded water molecules is suppressed.

In agreement with the results of TG analysis, the artificial aging significantly promotes the observed differences between the stable and unstable API system. Predominantly the ^{1}H-^{1}H correlation spectrum of the phase-stable system recorded after the accelerated aging displays more apparent and much stronger off-diagonal correlation signals (Figure 10c) indicating thus additional development and enhancement of the interaction network of hydrogen-bonded proton sites. In contrast, no correlation signals were fond in the spectrum recorded for the treated phase-unstable system. This indicates that the previously found traces of hydrogen-bonded clusters of H_2O are completely destroyed by the rearrangement of Si and Al tetrahedra during the accelerated aging. This finding is consistent with the assumption that water molecules become highly mobile within the pores and channels in zeolite crystals.

All these findings support our hypothesis that structural stability of AIP systems is connected with immobilization of water molecules. The experiments performed indicate that in the phase-stable systems strongly hydrated structures are formed. These structures are probably amorphous aluminosilicate hydrates that can be considered to be analogues of calcium-silicate-hydrate (C-S-H) gels of cements, in which water molecules are strongly bound to the inorganic substrate. It is well known that the strength of this binding is so strong that the release of water molecules requires very high temperature. The escape of this water is, however, accompanied by the total destruction of the gel [45,46]. On the basis of the above-mentioned results, we expect formation of similar strongly hydrated Al/Si/Na clusters in the phase-stable AIP systems. In these systems, even at relatively high temperatures, water molecules remain tightly bound and cannot provide liquid medium in which reactions of Na^+ ions with aluminosilicate matrix can take place. The immobilized Na^+ ions thus can not induce hydrolytic reactions and conversion of amorphous aluminosilicate phase to crystalline zeolites.

On the other hand, if these stable hydrated aluminosilicate clusters are not created in AIP systems and the interaction between water molecules and aluminosilicate matrix is weakened, then even slight temperature elevation converts the partly immobilized water from solid hydrates to liquid state. In the resulting highly alkaline medium, the presented dissociated ions (Na^+) attack Si-O-Al bonds to induce the conversion of stable amorphous phase to energetically more advantageous crystalline state. We suppose that exactly this process takes place in the phase-unstable system during artificial aging.

CONCLUSION

Aluminosilicate inorganic polymers (AIPs) that are currently of high significance to the building industry, sometimes exhibit undesired structural transformation from highly resistant amorphous state to the systems displaying high crystallinity with reduced mechanical properties. The presented study shows that structural stability of AIP systems can be controlled by the method of manufacture, while maintaining the overall chemical composition. It appears likely that the crucial step is activation of water glass, i.e. the moment of water addition into the reaction mixture. As shown, the different ways of activation of water glass results in different extent of hydration of primary aggregates involving aluminum and silica tetrahedra, and sodium ions. It was demonstrated that the extent of hydration of the inorganic matrix and the strength of binding of water into the inorganic framework affects structural stability of the prepared amorphous AIP systems.

Acknowledgment

The authors thank the Grant Agency of the Academy of Sciences of the Czech Republic (grant IAA400500602) and the Grant Agency of the Czech Republic (grant P108/10/1980) for financial support.

References

1. Gluchovskij V.D.: *Gruntosilicaty*, Grosstrojizdat Kijev 1959.
2. Davidovits J.: Journal of Thermal Analysis *37*, 1633 (1991).
3. Shi C., Stegemann J.A.: Cement and Concrete Research *30*, 803 (2000).
4. Davidovits J.: Journal of Materials Education *16*, 91 (1994).
5. Barbosa V.F.F., MacKenzie K.J.D.: Material Research Bulletin *38*, 319 (2003).
6. Barbosa V.F.F., MacKenzie K.J.D.: Materials Letters *57*, 1477 (2003).
7. van Jaarsveld J.G.S., van Deventer J.S.J.: Cement and Concrete Research *29*, 1189 (1999).
8. Phair J.W., van Deventer J.S.J.: Mineral Engineering *14*, 289 (2001).
9. van Jaarsveld J.G.S., van Deventer J.S.J., Lorenzen L.: Minerals Engineering *10*, 659 (1997).
10. van Jaarsveld J.G.S., van Deventer J.S.J., Schwartzman A.: Minerals Engineering *12*, 75 (1999).
11. Perera D.S., Blackford M.G., Vance E.R., Hanna J.V., Finnie K.S., Nicholson C.L.: Materials Research Society Symposium Proceeding *824*, 607 (2004).
12. Škvára F., Kopecký L., Němeček J., Bittner Z.: Ceramics-Silikaty *50*, 208 (2006).
13. Roy D.M.: Cement and Concrete Research, *29*, 249 (1999).
14. Sumajouw D.M.J., Hardjito D., Wallah S.E., Rangan B.V.: Journal of Material Science *42*, 3124 (2007).
15. Škvára F., Kopecký L., Myšková L., Šmilauer V., Alberovská L., Vinšová L.: Ceramics-Silikaty *53*, 276 (2009).

16. Minaříková M., Škvára F.: Ceramics-Silikaty *50*, 200 (2006)
17. Oudadesse H., Derrien A.C., Lefloch M., Davidovits J.: Journal of Material Science *42*, 3092 (2007).
18. Lyon R.E., Balaguru P.N., Foden A., Sorathia U., Davidovits J., Davidovics M.: Fire and Materials *21*, 67 (1997).
19. Barbosa V.F.F., MacKenzie K.J.D., Thaumaturgo C.: The International Journal of Inorganic Materials *2*, 309 (2000).
20. Duxson P., Lukey G.C., Separovic F., van Deventer J.S.J.: Industrial & Engineering Chemistry Research *44*, 832 (2005).
21. Duxson P., Lukey G.C., van Deventer J.S.J.: Journal of Materials Science *42*, 3044 (2007).
22. Sprygin A.I., Khoroshavin L.B., Ustyantsev V.M., Purgin A.K., Marevich V.P., Filin Y.A., Ivanov N.P., Tikhomirov A.V.: Refractories and Industrial Ceramics *23*, 30 (1982).
23. Singh P.S., Bastow T., Trigg M.: Journal of Material Science *40*, 3951 (2005).
24. Singh P.S., Trigg M., Burgar I., Bastow T.: Material Science Engineering, A: Properties, Microstructure and Processing *396*, 392 (2005)
25. Kolousek D., Brus J., Urbanova M., Andertova J., Hulinsky V., Vorel J.: Journal of Material Science *42*, 9267 (2007).
26. Provis J.L., Lukey G.C., van Deventer J.S.J.: Chemistry of Materials *17*, 3075 (2005)
27. Cournoyer R.A., Kranich W.L., Sand L.B.: The Journal of Physical Chemistry *79*, 1578 (1975).
28. Serrano D.P., van Grieken R.: Journal of Materials Chemistry *11*, 2391 (2001).
29. Bronić J., Subotić B.: Microporous Materials *4*, 239 (1995).
30. Ciric J.: Journal of Colloid and Interface Science *28*, 315 (1968).
31. Rahier H., Simons W., van Mele B., Biesemans M.: Journal of Materials Science *32*, 2237 (1997).
32. Duxson P., Fenandez-Jimenez A., Provis J.L., Lukey G.C., Palomo A., van Deventer J.S.J.: Journal of Material Science *42*, 2917 (2007).
33. Palomo A., Grutzeck M.W., Blanco M.T.: Cement and Concrete Research *29*, 1323 (1999).
34. Rowles M., O'Connor B.: Journal of Materials Chemistry *13*, 1161 (2003).
35. Duxson P., Mallicoat S.W., Lukey G.C., Kriven W.M., van Deventer J.S.J.: Colloids and Surfaces A: Physicochemical and Engineering Aspects *292*, 8 (2007).
36. Blackford M.G., Hanna J.V., Pike K.J., Vance E.R., Perera D.S.: Journal of the American Ceramic Society *90*, 1193 (2007).
37. Brus J., Karhan J., Kotlík P.: Collection of Czechoslovak Chemical Communications *61*, 691 (1996).
38. Brus J., Karhan J., Kotlík P.: Collection of Czechoslovak Chemical Communications *62*, 442 (1997).
39. Brus J.: Solid State Nuclear Magnetic Resonance *16*, 151 (2000).
40. Dai F., Deguchi K., Suzuki M., Takahashi H., Saito Y.: Chemistry Letters *17*, 869 (1988).
41. Deleuze M., Goiffon A., Ibanez A., Philippot E.: Journal of Solid State Chemistry *118*, 254 (1995).
42. Brus J., Dybal J.: Macromolecules *35*, 10038 (2002).
43. Brus J., Škrdlantová M.: Journal of Non-Crystalline Solid *281*, 61 (2001).
44. Brus J.: Journal of Sol-Gel Science and Technology *25*, 17 (2002).
45. Cong X., Kirkpatrick R.J.: Cement and Concrete Research *23*, 1065 (1993).
46. Stepkowska E.T., Blanes J.M., Real C., Perez-Rodriguez J.L.: Journal of Thermal Analysis and Calorimetry *82*, 731 (2005).